Superconducting $BaHfO_3$–$GdBa_2Cu_3O_7$ Nanocomposite Thin Films: Influence of Growth Temperature and Deposition Rate on Transport Properties

Ruslan Popov, Manuela Erbe, Jens Hänisch, and Bernhard Holzapfel

***Abstract*—Superconducting $GdBa_2Cu_3O_7$ films with 2.5 wt% of $BaHfO_3$ were deposited by pulsed laser deposition using an Nd:YAG laser ($\lambda = 355$ nm), and their structural and electrical properties were investigated in dependence of substrate temperature $T_{\rm sub}$ and deposition rate (i.e., laser repetition rate $\nu_{\rm dep}$). The irreversibility lines show the strongest shift toward higher magnetic fields at intermediate $T_{\rm sub}$ and lower $\nu_{\rm dep}$. The self-field J_c decreases by a factor of 2 compared with the pristine sample, but the situation improves in the high field region. The angular dependence of J_c at 1, 5, and 9 T shows a large *c*-axis peak at 180°, which indicates strongly correlated pinning at BHO nanocolumns.**

***Index Terms*—Critical current density, flux pinning, GdBCO, irreversibility field.**

I. Introduction

IN THE last decades, high temperature superconductors (HTS) were investigated with regard to many possible applications in electrical engineering, such as motors and generators, and also in superconducting electronics. One of the promising materials are $RE$$Ba_2Cu_3O_7$ (*RE*BCO, *RE* = rare earth) superconducting thin films. *RE*BCO superconducting thin films are characterized by high critical temperatures (T_c) and relatively high critical current densities (J_c) in magnetic fields, which is even more important for engineering applications. One of the features of *RE*BCO films is that they contain growth related defects and may also contain additionally introduced defects with different shape and dimensionality. J_c in HTS is defined by the interaction of the flux lines with those defects which act as pinning centers. Thus, by the introduction of artificial pinning centers (APCs) it is possible to further improve in-field characteristics of superconductors.

Many studies were dedicated to the introduction of defects by different approaches (heavy-ion irradiation etc.). However, one of the best results has been presented by pulsed-laser deposited *RE*BCO films with $BaMO_3$ (M = Hf, Sn, Zr) addition. As shown by MacManus-Driscoll *et al.* [1], the addition of $BaZrO_3$ (BZO) leads to the heteroepitaxial growth of BZO nanoparticles with the YBCO matrix which in turn increases in-field J_c by a factor of 1.5–5.

Shortly after, Goyal A. *et al.* [2] and Y. Yamada *et al.* [3] showed that secondary phase additions in YBCO, such as BZO and YSZ, can form columnar structures, which act as effective pinning centers and improve in-field transport properties of *RE*BCO superconducting thin films.

The morphology of defects is defined by the growth kinetics. Therefore, for a certain J_c improvement the dependence of the nanoparticle formation on growth conditions is important, mainly the deposition temperature $T_{\rm dep}$ and the growth rate, i.e., here the laser repetition rate $\nu_{\rm dep}$. As shown by different studies of e.g., Y. Ichino *et al.* B. Maiorov *et al.* and G. Ercolano *et al.* [4]–[6] $T_{\rm dep}$ affects size, shape and orientation distribution of the nanoparticles, and $\nu_{\rm dep}$ influence density and shape of the nanoparticles. As an example, in the work of B. Maiorov *et al.* [5] the film grown at low $T_{\rm dep}$ and high $\nu_{\rm dep}$ have a combination of nanoparticles and short nanocolumns which can be effective pinning centers only in low magnetic fields. Based on these reasons it is important to clarify the optimum deposition parameters to achieve highest J_c at a certain magnetic field.

In this work, we investigate the influence of the deposition conditions on microstructure and superconducting properties of 2.5 wt% $BaHfO_3$-containing $GdBa_2Cu_3O_7$ nanocomposite. The use of GdBCO as matrix for the nanoparticle growth is based on its higher T_c and in general higher J_c values compared to YBCO. As reported by K. Takahashi *et al.* [7], YBCO and GdBCO films with thickness of 200 nm do not show significantly different self-field J_c values at 77 K. However, it is 2 times higher for GdBCO in thicker films. Moreover, as shown by T. Horide *et al.* [8], BHO nanoparticles suppress self-field J_c more strongly than BZO and BSO, however show better in-field improvement and, as reported by H. Tobita *et al.* [9], a more isotropic field orientation dependence in GdBCO independent of the film thickness.

Manuscript received October 30, 2018; accepted January 2, 2019. Date of publication January 22, 2019; date of current version February 4, 2019. This work was supported by KSETA Graduate School. (*Corresponding author Ruslan Popov*.)

The authors are with the Institute for Technical Physics, Karlsruhe Institute of Technology, Eggenstein-Leopolshafen 76344, Germany (e-mail: ruslan.popov@kit.edu).

Color versions of one or more of the figures in this paper are available online at http://ieeexplore.ieee.org.

Digital Object Identifier 10.1109/TASC.2019.2892039

TABLE I
BASIC CHARACTERISTICS OF PRISTINE AND 2.5 WT% BHO CONTAINING GDBCO FILMS

	Pristine	780 °C, 10 Hz	800 °C, 10 Hz	820 °C, 10 Hz	840 °C, 10 Hz
T_c, K	92.5	90.28	91.79	92.03	91.68
$J_c(0)$ at 77 K, MA/cm^2	3.08	1.52	1.44	0.89	0.78
$F_{p,max}$ at 77 K, GN/m^3	4.6	3.2	6.4	6.6	2.5
$F_{p,max}$ at 65 K, GN/m^3	12.6	25.4	45.7	34.6	23.5

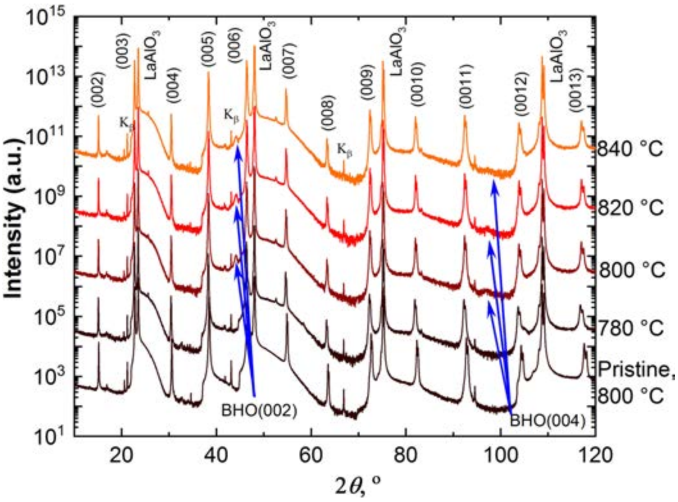

Fig. 1. θ-2θ scans of PLD-grown 2.5 wt% BHO-GdBCO nanocomposite films on LAO substrate deposited at several temperatures between 780 °C and 840 °C ($\nu_{\mathrm{dep}} = 10$ Hz) compared to a pristine sample. GdBCO (00*l*) peaks with BHO (002) are present at $T_{\mathrm{sub}} = 800$ °C–840 °C. Small (*h*00) peaks appear at 780 °C.

II. EXPERIMENTS

BHO-GdBCO nanocomposite films were grown on $LaAlO_3$ (100) (LAO) single crystals by pulsed laser deposition from mixed targets of GdBCO with 2.5 wt% (2 vol.%) BHO using a 3rd harmonic Nd - YAG laser ($\lambda = 355$ nm). During the deposition, the laser energy density at the spot of 2 mm diameter on the target was around 2 J/cm^2. The substrate temperature was controlled by a thermocouple inserted in the heater and varied between 780 °C and 840 °C, the laser repetition rate was set to 1 Hz, 2 Hz, 5 Hz and 10 Hz for nanocomposite GdBCO films, while for pristine samples 800 °C, 10 Hz have been found to be the optimum. The oxygen partial pressure was kept at 40 Pa. After the deposition, all samples were cooled down by 20 °C from the deposition temperature and annealed at 400 mbar in the oxygen atmosphere during further cool-down till room temperature. All films were deposited with 6000 pulses and resulting film thicknesses were around 200–220 nm. Critical temperatures were measured resistively and determined with a criterion 10% of the normal state resistance, and microstructure as well as phase purity of the films were investigated by x-ray diffraction (XRD) using a Bruker D8 diffractometer with Cu Kα radiation. After initial characterization, microbridges of 1 mm length and 20–30 μm width were patterned by photolithography and wet-chemical etching. Transport properties were measured in a Quantum Design PPMS with 14 T maximum field at different magnetic fields and orientations in maximum Lorentz force configuration. J_c was determined with 1 μV/cm electrical field criterion and the irreversibility temperatures were determined with constant resistance criterion of $R(\mathrm{T})/R(100\mathrm{K}) \approx 10^{-7}$.

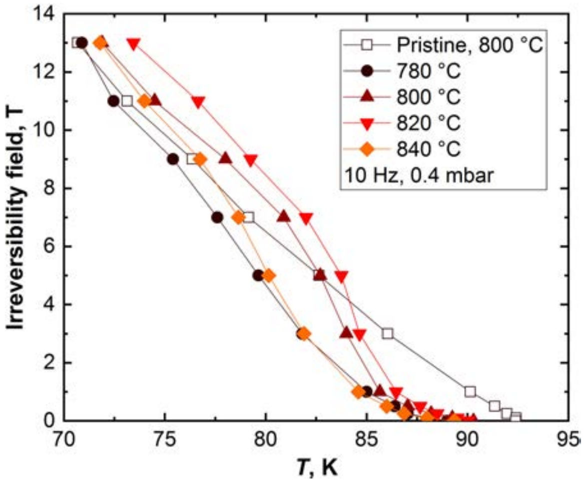

Fig. 2. Temperature dependence of the irreversibility field for 2.5 wt% BHO GdBCO nanocomposite films deposited at 780 °C −840 °C and 10 Hz compared to pristine sample.

III. RESULTS

A. Influence of the Substrate Temperature

Table I shows the basic properties for of the pristine and 2.5 wt% BHO-containing GdBCO films deposited on LAO substrate at 780 °C−840 °C and a laser repetition rate of 10 Hz. As can be seen, pristine sample have slightly higher T_c and 2 times higher self-field J_c values, which is common for the introduction of secondary phases into *RE*BCO by PLD. Nevertheless, due to formation of BHO nanocolumns in GdBCO the in-field characteristics are improved. The maximum pinning force densities $F_{\mathrm{p,max}}$ for the pristine film are 4.6 GN/m^3 at 77 K and 12.6 GN/m^3 at 65 K while the highest $F_{\mathrm{p,max}}$ achieved with 2.5 wt% BHO are 6.6 GN/m^3 at 77 K for the sample at 820 °C and 45.7 GN/m^3 at 65 K for the sample at 800 °C. For applications it is important to ensure that all pristine and nanocomposite GdBCO films are *c*-axis-oriented. As can be seen in Fig. 1, the pristine GdBCO sample and GdBCO+2.5 wt% BHO samples grown at different temperatures show only (00*l*) peaks indicating that the films are highly *c*-axis oriented, moreover BHO (002) at $2\theta \approx 44°$ and (004) at $2\theta \approx 96°$ are clearly present.

The irreversibility lines (IL), i.e., transition between vortex glass and vortex liquid, on the Fig. 2 show clear differences for different substrate temperatures for 10 Hz and $T_{\mathrm{sub}} = 780$ °C–840 °C. The ILs for 800 °C and 820 °C show an S-shape and a more or less linear part at low *T*, which is a clear sign of correlated pinning centers with matching field $B_\Phi \approx 6.5$ T at 800 °C and $B_\Phi \approx 6$ T at 820 °C.

The magnetic field dependence of J_c for $B \| c$ shows a crossover between the pristine sample and nanocomposites. Fig. 3 the

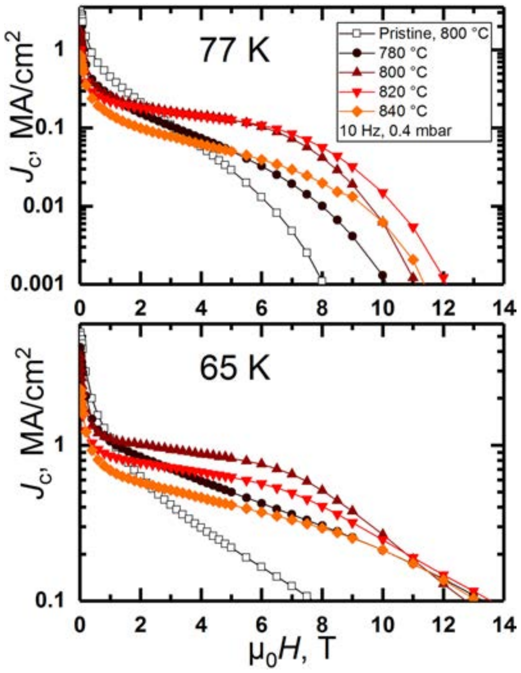

Fig. 3. Field dependence of the critical current density, $J_c(B)$, characteristics of 2.5 wt% BHO containing GdBCO films grown on LAO substrate at different temperatures between 780 and 840 °C and a repetition rate of 10 Hz compared to a pristine film.

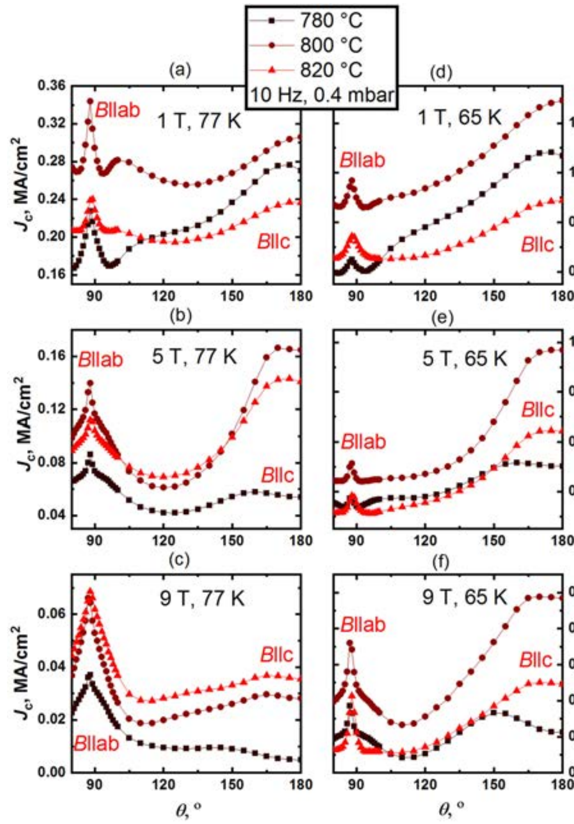

Fig. 4. J_c-θ dependence of 2.5 wt% BHO containing GdBCO films deposited on LAO substrate at 780 °C–820 °C with 10 Hz. (a)–(c)77 K 1 T, 5 T and 9 T. (d)–(f) 65 K 1 T, 5 T and 9 T.

pristine film has the highest self-field J_c around 3.1 MA/cm^2, but the in-field J_c is decreasing strongly with magnetic field, while nanocomposite samples show a much slower decrease in fields above 2 T. At liquid nitrogen temperatures and in field region above 5 T, the samples grown at 780 °C and 840 °C also show larger J_c values compared to the pristine sample, however they show a stronger field dependence compared to the samples grown at medium temperatures.

*RE*BCO superconducting thin films are known for a strong anisotropy of the critical current density regarding the filed direction. Pristine GdBCO films show a peak in J_c for magnetic field parallel to the *ab*-planes and often a small peak in the *c*-direction is present as well, which can appear due to defects such as stacking faults effective in the *c*-direction [10], [11]. Fig. 4 compares the $J_c(\theta)$ dependencies (θ–angle between *B* and *c*-axis) of samples grown at 780 °C–820 °C and 10 Hz at 77 K (a–c) and 65 K (d–f) in 1 T, 5 T and 9 T. As can be seen there is a large broad peak at all magnetic fields which indicates strong correlated pinning on BHO nanocolumns.

B. Influence of the Deposition Rate

Another important deposition parameter is the deposition rate, varied here via the laser repetition rate (v_{dep}). After optimization of the deposition temperature as shown above, the highest J_c values were achieved for the samples at 800 °C and 820 °C. For further improvement of the pinning and transport properties we deposited 2.5 wt% BHO containing GdBCO films at 800 °C also with 5 and 2 Hz. All samples have GdBCO (00*l*) peaks (not shown) which indicates that the films are highly *c*-axis oriented. Moreover, the BHO (002) peaks are present and BHO (004) has a higher intensity at 5 and 2 Hz. ILs for the samples prepared at different v_{dep} (not shown) shows S–shape similar to the sample at 10 Hz and further shift toward higher magnetic fields for the 5 Hz. However, for the sample at 2 Hz, this type of curvature is not clearly visible.

The magnetic field dependence of J_c for these films is shown in Fig. 5. The samples grown at 10 Hz and 5 Hz have similar self–field J_c values of 1.40 MA/cm^2 and 1.39 MA/cm^2. In the whole field range, the 5 Hz sample has the highest J_c values, which indicates more effective pinning centers are introduced at lower v_{dep}. A similar behavior is seen at 65 K. The highest pinning force densities were reached so far for the sample grown at 5 Hz with values of 11 GN/m^3 at 77 K and 54.6 GN/m^3 at 65 K.

Fig. 6 compares the $J_c(\theta)$ dependence for the samples grown at 10 Hz and 5 Hz. In correspondence with Fig. 5, the 5 Hz sample has higher J_c values. Moreover, similar to the 10 Hz sample the broad peak at 180º is present at all magnetic fields as well as the flat region around the *c*-direction.

IV. Discussions

As can be seen from Table I, the introduction of the secondary phases slightly decreases T_c of the GdBCO films which is mainly caused by the strain induced by nanocolumns and surrounding regions with oxygen deficiency. This further leads to decrease of the self-field J_c. A similar trend has been reported

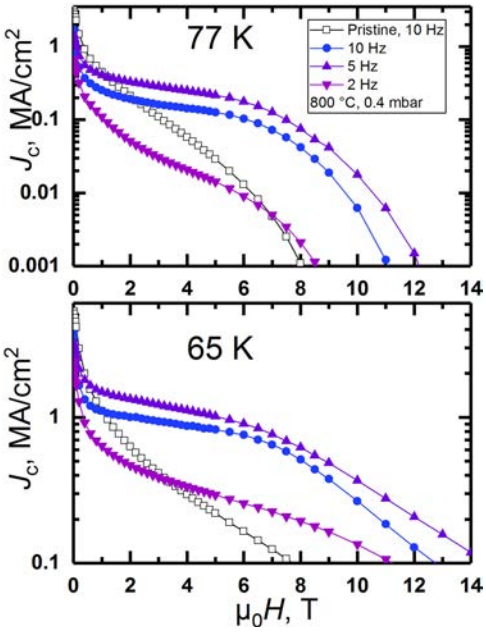

Fig. 5. Field dependence of the critical current density, $J_c(B)$, of 2.5 wt% BHO containing GdBCO films deposited on LAO substrate at 800 °C with 2, 5, and 10 Hz compared to a pristine film.

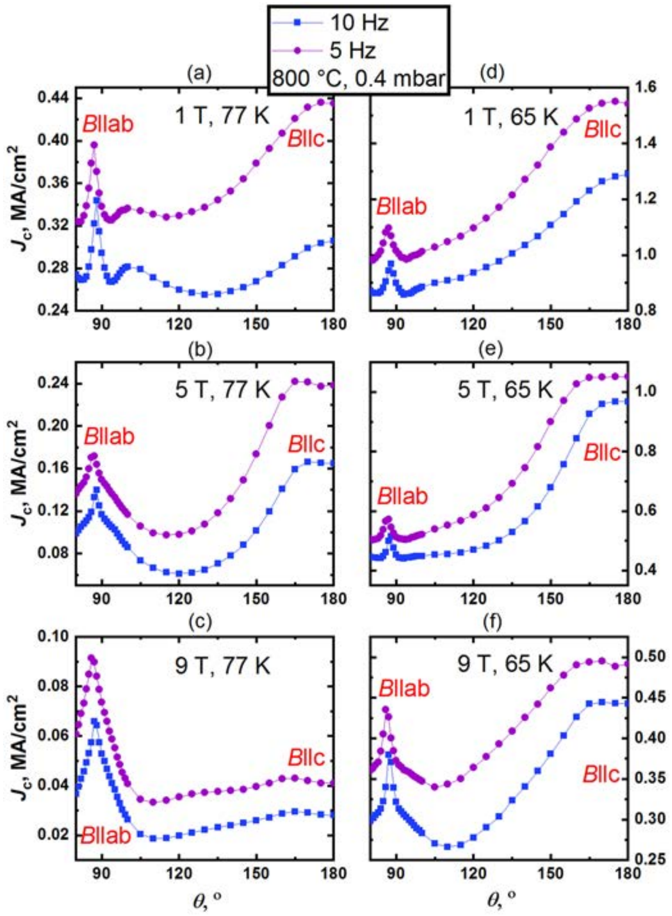

Fig. 6. J_c-θ dependence of 2.5 wt% BHO containing GdBCO films deposited on LAO substrate at 800 °C with 10, 5. (a)–(c) 77 K at 1 T, 5 T and 9 T. (d)–(f) 65 K at 1 T, 5 T and 9 T.

by K. Ko *et al.* [12] on GdBCO films with different amounts of $BaSnO_3$ on CeO_2-buffered IBAD-MgO templates.

The S-shape of the irreversibility line (IL) (Fig. 2), which is similar to results shown in refs. [13], [14], indicates that BHO forms nanocolumns in GdBCO at higher substrate temperatures (800 °C and 820 °C), and this is based on the low lattice mismatch between GdBCO and BHO which induces elongated vertical growth of BHO, as it can be seen in the refs. [15], [16]. However, this S-shape is not clearly visible for 840 °C and 780 °C which might be due to the formation of short nanocolumns and nanoparticles. In many studies it was shown that at low deposition temperatures BHO and BZO form short nanocolumns and nanoparticles [4], [5]. An increase of the deposition temperature first leads to inclined nanorods and further to more straight ones with bigger size, but lower density. Estimated B_Φ at 800 °C and 820 °C also confirms a decrease of the density of the nanocolumns. The deposition rate (here laser repetition rate $v_{\rm dep}$) has a similar effect on the shape and size of the nanocolumns. Ichino *et al.* [4] showed by 3D Monte-Carlo simulations that the highest density of defects can be achieved at higher $v_{\rm dep}$. In our case, B_Φ has same values for the sample at 800 °C but with 10 Hz and 5 Hz frequencies. This shows that decrease in $v_{\rm dep}$ increases diffusion time and leads to a better alignment of the columnar defects. Further decrease of the $v_{\rm dep}$ only increases the size of the defects and thus the S-shape curvature is not clearly seen for IL of 2 Hz sample.

In accordance with ILs, possibly due to formation of the most well aligned nanocolumns, the sample grown at 820 °C has a rather low self-field J_c but the highest in-field J_cs at 77 K. A similar behavior with slightly lower J_c is found for the sample grown at 800 °C, which however takes over at 65 K and below. Further improvement of the in-field J_c values at 800 °C was achieved through decrease of $v_{\rm dep}$. The dependence of J_c on $v_{\rm dep}$ shown in Fig. 5 is similar to results of Maiorov *et al.* [5] for BZO-YBCO films deposited at 10 Hz, 5 Hz and 2 Hz. Also there, the highest J_c values were achieved at a frequency of 5 Hz. The highest achieved $F_{\rm p,max}$ so far in our samples are comparable with those reported by P. Cayado *et al.* [17], for CSD-grown GdBCO films with 12 mol% BHO, however they are lower by a factor of 2 in comparison with work of S. Awaji *et al.* [18], for 1.5vol% BHO-containing GdBCO films grown by PLD on tapes.

In Figs. 4 and 6 broad peaks in the *c*-direction indicates that BHO nanocolumns act as effective pinning centers in $B||c$. The flat regions around 180° are most likely due to inclined and splayed BHO nanocolumns, but this needs to be further investigated by TEM.

V. Conclusion

In order to investigate the influence of growth temperature and deposition rate on the nanocolumn formation in 2.5 wt% BHO-GdBCO nanocomposite films and their transport properties, such films were deposited at 780 °C–840 °C with 10 Hz and at 800 °C with 2 and 5 Hz. Comparison with pristine GdBCO films showed significant improvement of in-field J_c in magnetic fields up to 11 T. With optimum growth temperature and deposition rate we achieved a maximum pinning force density $F_{p,max} = 11$ GN/m^3 at 77 K and 54.6 GN/m^3 at 65 K. The $J_c(\theta)$ dependence shows that the introduction of BHO improves pinning properties of the GdBCO films and they act as effective pinning centers in the *c*-axis direction.

Acknowledgment

We would like to thank A. Gruber for technical assistance, P. Cayado-Llosa, K. Ackermann, M. Langer and S. Meyer for the numerous discussions.

References

[1] J. L. MacManus-Driscoll *et al.*, "Strongly enhanced current densities in superconducting coated conductors of $YBa_2Cu_3O_{7-x}$+$BaZrO_3$," *Nat. Mater.*, vol. 3, pp. 439–433, 2004.

[2] A. Goyal *et al.*, "Irradiation-free, columnar defects comprised of self-assembled nanodots and nanorods resulting in strongly enhanced flux-pinning in $YBa_2Cu_3O_{7-\delta}$ films," *Supercond. Sci. Technol*, vol. 18, pp. 1533–1538, 2005.

[3] Y. Yamada *et al.*, "Epitaxial nanostructure and defects effective for pinning in Y(*RE*)$Ba_2Cu_3O_{7-x}$ coated conductors," *Appl. Phys. Lett.*, vol. 87, 2005, Art. no. 132502.

[4] Y. Ichino, Y. Yoshida, and S. Miura, "Three-dimensional Monte Carlo simulation of nanorod self-organization in $REBa_2Cu_3O_y$ thin films grown by vapor phase epitaxy," *Jpn. J. Appl. Phys.*, vol. 56, 2017, Art. no. 015601.

[5] B. Maiorov *et al.*, "Synergetic combination of different types of defect to optimize pinning landscape using $BaZrO_3$-doped $YBa_2Cu_3O_7$," *Nat. Mater.*, vol. 8, pp. 398–404, 2009.

[6] G. Ercolano *et al.*, "Strong correlated pinning at high growth rates in $YBa_2Cu_3O_{7-x}$ thin films with Ba_2YNbO_6 additions," *J. Appl. Phys.*, vol. 116, 2014, Art. no. 033915.

[7] K. Takahashi *et al.*, "Investigation of thick PLD-GdBCO and ZrO_2 doped GdBCO coated conductors with high critical current on PLD-CeO_2 capped IBAD-GZO substrate tapes," *Supercond. Sci. Technol.*, vol. 19, pp. 924–929, 2006.

[8] T. Horide *et al.*, "Influence of matching field on critical current density and irreversibility temperature in $YBa_2Cu_3O_7$ films with $BaMO_3$(M = Zr, Sn, Hf) nanorods," *Appl. Phys. Lett.*, vol. 108, 2016, Art. no. 082601.

[9] H. Tobita *et al.*, "Fabrication of $BaHfO_3$ doped $GdBa_2Cu_3O_{7-\delta}$ coated conductors with the high I_c of 85A/cm-w under 3T at liquid nitrogen temperature (77K)," *Supercond. Sci. Technol.*, vol. 25, 2012, Art. no. 062002.

[10] K. Takahashi *et al.*, "Magnetic field dependence of J_c for Gd-123 coated conductors on PLD-CeO_2 capped IBAD-GZO substrate tapes," *Supercond. Sci. Technol.*, vol. 18, pp. 1118–1122, 2005

[11] K. Matsumoto *et al.*, "High-J_c Gd-Ba-Cu-O epitaxial films prepared by pulsed laser deposition," *IEEE Trans. Appl. Supercond.*, vol. 15, no. 2, pp. 2719–2722, Jun. 2005.

[12] K. Ko *et al.*, "Optimization of the $BaSnO_3$ doping content in $GdBa_2Cu_3O_{7-\delta}$ coated conductors by pulsed laser deposition," *IEEE Trans. Appl. Supercond.*, vol. 24, no. 6, Dec. 2014, Art. no. 6600908.

[13] T. Horide *et al.*, "Matching field effect of the vortices in $GdBa_2Cu_3O_{7-\delta}$ thin film with gold nanorods," *Supercond. Sci. Technol.*, vol. 20, pp. 303–306, 2007.

[14] T. Horide *et al.*, "Control of the glass-liquid transition temperature in $YBa_2Cu_3O_{7-x}$ films," *Phys. Rev.*, vol. 79, 2009, Art. no. 092504.

[15] M. H. Gharahcheshmeh *et al.*, "Control of in-field performance of 25 mol% Zr-added *RE*BCO superconductor tapes," *Physica C*, vol. 553, pp. 26–32, 2018.

[16] J. J. Shi and J. Z. Wu, "Micromechanical model for self-organized secondary phase oxide nanorod arrays in epitaxial $YBa_2Cu_3O_{7-\delta}$ films," *Philos. Mag.*, vol. 92, pp. 2911–2922, 2012.

[17] P. Cayado *et al.*, "Large critical current densities and pinning forces in CSD-grown superconducting $GdBa_2Cu_3O_{7-x}$-$BaHfO_3$ nanocomposite films," *Supercond. Sci. Technol.*, vol. 30, 2017, Art. no. 094007.

[18] S. Awaji *et al.*, "High-performance irreversibility field and flux pinning force density in $BaHfO_3$-doped $GdBa_2Cu_3O_y$ tape prepared by pulsed laser deposition," *Appl. Phys. Express*, vol. 8, 2015, Art. no. 023101.